Title

Common and Divergent Features of Galactose-1-phosphate and Fructose-1-phosphate Toxicity in Yeast

Journal

Molecular Biology of the Cell, 29(8)

ISSN

1059-1524

Authors

Gibney, Patrick A

Schieler, Ariel

Chen, Jonathan C

et al.

Publication Date

2018-04-15

DOI

10.1091/mbc.e17-11-0666

Common and divergent features of galactose-1-phosphate and fructose-1-phosphate toxicity in yeast

Patrick A. Gibney[a,b,c,*], Ariel Schieler[a], Jonathan C. Chen[a,d], Jessie M. Bacha-Hummel[e,†], Maxim Botstein[a,†], Matthew Volpe[a,†], Sanford J. Silverman[a], Yifan Xu[a,d], Bryson D. Bennett[b], Joshua D. Rabinowitz[a,d], and David Botstein[a,b,c]

[a]Lewis-Sigler Institute for Integrative Genomics and [d]Department of Chemistry, Princeton University, Princeton, NJ 08544; [b]Calico Life Sciences LLC, South San Francisco, CA 94080; [c]Department of Food Science, Cornell University, Ithaca, NY 14853; [e]Biology Department, Swarthmore College, Swarthmore, PA 19081

ABSTRACT **Toxicity resulting from accumulation of sugar-phosphate molecules is an evolutionarily conserved phenomenon, observed in multiple bacterial and eukaryotic systems, including a number of human diseases. However, the molecular mechanisms involved in sugar-phosphate toxicity remain unclear. Using the model eukaryote *Saccharomyces cerevisiae*, we developed two systems to accumulate human disease-associated sugar-phosphate species. One system utilizes constitutive expression of galactose permease and galactose kinase to accumulate galactose-1-phosphate, while the other system utilizes constitutive expression of a mammalian ketohexokinase gene to accumulate fructose-1-phosphate. These systems advantageously dissociate sugar-phosphate toxicity from metabolic demand for downstream enzymatic products. Using them, we characterized the pathophysiological effects of sugar-phosphate accumulation, in addition to identifying a number of genetic suppressors that repair sugar-phosphate toxicity. By comparing the effects of different sugar-phosphates, and examining the specificity of genetic suppressors, we observed a number of striking similarities and significant differences. These results suggest that sugar-phosphates exert toxic effects, at least in part, through isomer-specific mechanisms rather than through a single general mechanism common to accumulation of any sugar-phosphate.**

Monitoring Editor
David G. Drubin
University of California, Berkeley

Received: Nov 27, 2017
Revised: Jan 24, 2018
Accepted: Feb 8, 2018

INTRODUCTION

Accumulation of a great diversity of sugar-phosphate molecules inside cells has been connected to growth inhibition in species ranging from bacteria to humans. In bacteria this has been widely studied using mutations in various biosynthetic pathways that lead to toxic sugar-phosphate accumulation, including phosphorylated ribulose, glucose, fructose, mannose, arabinose, galactose, and glucosamine (Fukasawa and Nikaido, 1959; Yarmolinsky *et al.*, 1959; Englesberg *et al.*, 1962; Kadner *et al.*, 1992; Lyngstadaas *et al.*, 1998). Sugar-phosphate accumulation can be recapitulated by various genetic perturbations in *Saccharomyces cerevisiae* as well. For example, cells are unable to grow using galactose in strains lacking galactose-1-phosphate uridyl transferase (*GAL7*), presumably due to the accumulation of galactose-1-phosphate (Douglas and Hawthorne, 1964). Additionally, overexpression of xylulokinase in yeast causes production of xylulose-phosphate and inhibits cell growth (Rodriguez-Pena *et al.*, 1998; Jin *et al.*, 2003). Beyond yeast, a number of recessive metabolic diseases in humans have been linked to mutations that result in accumulation of toxic sugar-phosphates, including galactose-1-phosphate in classic galactosemia (due to mutation of GALT, the human homolog of yeast *GAL7*) or fructose-1-phosphate in hereditary fructose intolerance (due to mutation of ALDOB, aldolase B) (Herman and Zakim, 1968; Froesch, 1969;

This article was published online ahead of print in MBoC in Press (http://www.molbiolcell.org/cgi/doi/10.1091/mbc.E17-11-0666) on February 12, 2018.

†These authors contributed equally to this work.

Author contributions: P.G. and D.B. designed research; P.G., A.S., J.C., J.B., M.B., M.V., S.S., Y.X., and B.B. performed research and analyzed data; P.G., A.S., J.C., J.B., M.B., M.V., S.S., Y.X., B.B., J.R., and D.B. wrote the article.

*Address correspondence to: Patrick Gibney (pag235@cornell.edu).

Abbreviations used: 2DG, 2-deoxyglucose; ESR, environmental stress response; Fru1P, fructose-1-phosphate; Gal1P, galactose-1-phosphate.

Petry and Reichardt, 1998; Lai *et al.*, 2009). It is also possible that, in the general population, fructose-1-phosphate accumulation contributes to adverse health outcomes associated with dietary fructose, that is, a reason why sweets are less healthy than other carbohydrates.

Despite widespread observations of sugar-phosphate toxicity, the molecular mechanism behind these observations remains unclear. One hypothesis is that accumulation of sugar-phosphates causes general changes such as interruption of membrane integrity, change in cellular pH, depletion of inorganic phosphate, or widespread glycation of proteins in the cell. An alternative hypothesis is that specific sugar-phosphates inhibit specific cellular processes, such as enzymes involved in inositol metabolism, RNA metabolism, phosphoglucomutase activity, uridine diphosphate (UDP) hexose production, and so on (Mehta *et al.*, 1999; Lai *et al.*, 2003; Slepak *et al.*, 2005; de Jongh *et al.*, 2008). The former hypothesis suggests a common effect for all sugar-phosphates, while the latter hypothesis suggests that individual types of sugar-phosphates have different mechanisms of toxicity.

Saccharomyces cerevisiae has been successfully used as a model for eukaryotic cell biology for decades due to homology of cellular processes throughout all eukaryotes (Botstein and Fink, 2011). Notably, deletion of *GAL7* has been used to model the effects of classic galactosemia and to identify potential suppressors that could inform treatment of the human disease (Mehta *et al.*, 1999; Lai and Elsas, 2000; de Jongh *et al.*, 2008; Masuda *et al.*, 2008; De-Souza *et al.*, 2014). Additionally, potential causative alleles of classic galactosemia have been tested in yeast to confirm whether they are truly loss-of-function mutations, an approach that is becoming more common after multiple successes including examining potential cancer-causing disease alleles of DNA mismatch repair in yeast (Gammie *et al.*, 2007; Lang *et al.*, 2013; Sirr *et al.*, 2015).

Attempts to examine the direct effects of accumulated sugar-phosphates on cell biology are confounded by the perturbations required to produce sugar-phosphates. These perturbations are often mutations in a metabolic pathway. These mutations tend to have additional metabolic effects, including an accumulation of sugar-phosphates before the metabolic block but also a decrease in metabolites after the metabolic block. To circumvent this, we developed two systems in yeast to accumulate different sugar-phosphates using a mechanism that does not inherently affect downstream metabolism. In both cases, the sugar being used as a precursor for sugar-phosphate accumulation is not necessary for cellular growth nor is it the preferred carbon source present in the growth medium. We used each of these systems to characterize the physiological effects of galactose-1-phosphate (Gal1P) or fructose-1-phosphate (Fru1P) accumulation and to identify genetic suppressors of their toxicity. By identifying suppressor mutations and examining their ability to cross-suppress against other sugar-phosphates, we showed that despite some striking similarities, there are multiple differences suggesting that the mechanisms by which these two sugar-phosphates inhibit growth are different.

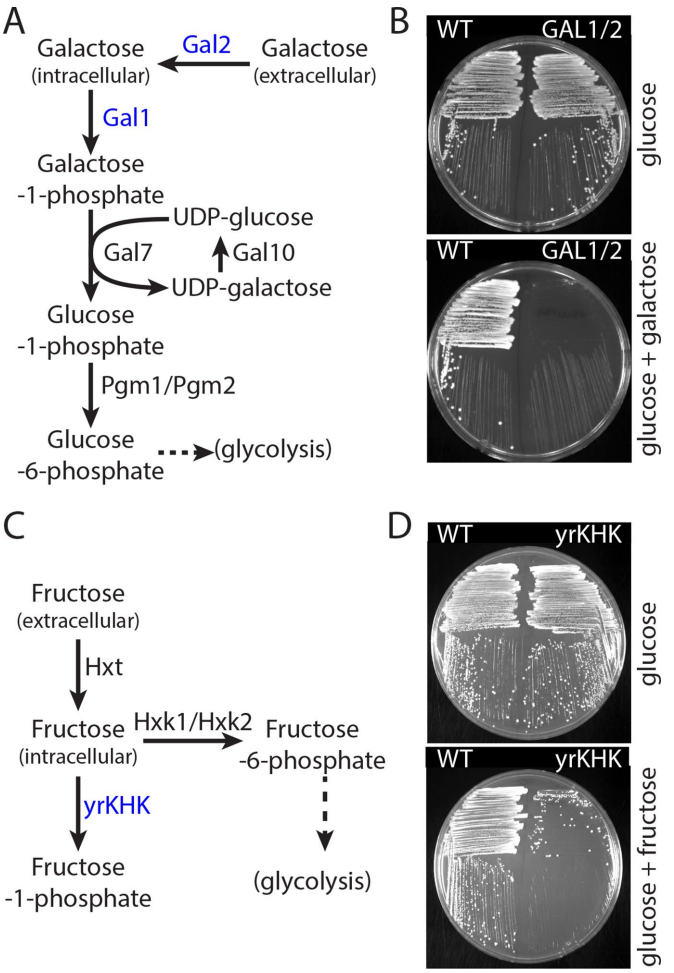

FIGURE 1: Development of independent systems to accumulate galactose-1-phosphate or fructose-1-phosphate. (A) Schematic of galactose metabolism; genes constitutively expressed by the *TDH3* promoter are highlighted in blue. (B) WT and GAL1/2 cells were struck out onto YNB + 2% glucose or YNB + 2% glucose + 2% galactose, as indicated. Plates were incubated for 2 d at 30°C. (C) Schematic of fructose metabolism; mammalian liver ketohexokinase gene constitutively expressed by the *TDH3* promoter is highlighted in blue. (D) WT and yrKHK cells were struck out onto YNB + 2% glucose or YNB + 2% glucose + 2% fructose, as indicated. Plates were incubated for 2 d at 30°C.

RESULTS

Development of in vivo models for galactose-1-phosphate and fructose-1-phosphate accumulation

To better understand how accumulation of sugar-phosphate molecules results in toxicity, we developed two independent systems in the model eukaryote *S. cerevisiae*. The first allows glucose-grown cells with added galactose to accumulate Gal1P. This is accomplished by the constitutive overexpression (using the *TDH3* promoter from the glyceraldehyde-3-phosphate dehydrogenase gene) of both the *GAL2* (galactose permease) and *GAL1* (galactose kinase) genes (Figure 1A). This strain (termed "GAL1/2") grows normally on glucose-containing medium, but growth is inhibited in medium with galactose present (even when glucose is also present) (Figure 1B). Previous models of galactosemia in yeast have used mutations of *GAL7* that exhibit functional consequences only when cells are grown on galactose (Mehta *et al.*, 1999; Lai and Elsas, 2000; de Jongh *et al.*, 2008; Masuda *et al.*, 2008; De-Souza *et al.*, 2014). In contrast, our strain exhibits galactosemic phenotypes even in the presence of glucose. This isolates the accumulation of galactose-1-phosphate from a requirement for galactose metabolism and mimics the situation in mammals, where galactosemia is not prevented by the nearly constant level of glucose available in the blood.

The second system utilizes expression of a mammalian fructokinase to produce Fru1P. Normally, fructose catabolism in yeast produces the glycolytic intermediate fructose-6-phosphate; in

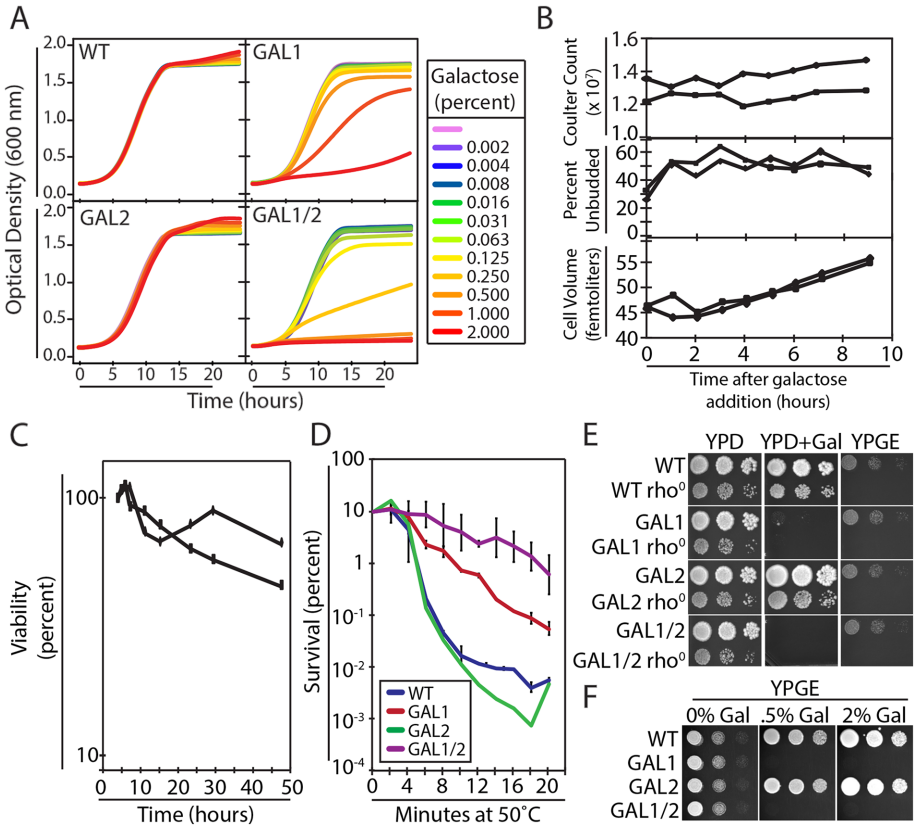

FIGURE 2: Physiological effects of galactose-1-phosphate accumulation. (A) Dose–response curves of indicated strains in YPD at 30°C with indicated concentrations of galactose added (replicates and dose–response curves in different media are shown in Supplemental Figure 1). (B) GAL1/2 cells were grown to early log phase in YNB + 2% glucose before galactose was added to 2% at time zero. Cell volume and particle count were measured every hour with a Coulter counter. Percentage of unbudded cells was measured every hour with a hemocytometer. Each line represents an independent biological replicate. (C) GAL1/2 homozygous diploid cells were grown to early log phase in YNB + 2% glucose before galactose was added to 2% at 4 h. Survival at indicated time points was assessed by plating and counting CFU on YPD plates. Each line represents an independent biological replicate. (D) Indicated strains were grown to log phase in YNB + 2% glucose before galactose was added to 2% for 2 h. Cells were then subjected to a 50°C heat shock, and samples were taken every 2 min and plated onto YPD to count CFU. Error bars represent SD of two biological replicates. (E) Tenfold serial dilutions of indicated strains were spotted onto YP medium containing either 2% glucose (YPD), 2% glucose, and 2% galactose (YPD+Gal) or 3% glycerol and 2% ethanol (YPGE), as indicated. Cell density in initial spot was normalized to an OD_{600} = 1.0. Plates were incubated for 2 d at 30°C. (F) Tenfold serial dilutions of indicated strains were spotted onto YPGE plates containing indicated amounts of galactose. Cell density in initial spot was normalized to an OD_{600} = 1.0. Plates were incubated for 2 d at 30°C.

mammalian liver cells, however, fructose is phosphorylated to Fru1P by ketohexokinase (KHK) (Figure 1C). We therefore expressed a yeast-codon-optimized version of rat liver ketohexokinase using the *TDH3* promoter, with the expectation that addition of fructose to the medium of growing cells would result in accumulation of Fru1P, a metabolite not normally present in yeast. This is an adaptation from a construct first made to study mutant versions of invertase in yeast (Donaldson *et al.*, 1993; Doyle *et al.*, 1993). This strain (termed "yrKHK") grows normally on glucose-containing medium, though growth is inhibited when fructose is present (Figure 1D).

Notably, when streaking the yrKHK strain onto fructose-containing medium, or when streaking the GAL1/2 strain onto galactose-containing medium, we often observed suppressors in the primary streak (Figure 1). Suppression analysis (described below) indicated that the vast majority of suppressors are inactivating mutations in the constitutively expressed genes responsible for the accumulation of the sugar-phosphates.

Physiological characterization of galactose-1-phosphate accumulation

We first sought to identify the concentrations of galactose that exhibit toxicity in our system. To this end, growth curves were performed in glucose-containing media with variable amounts of galactose present (Figure 2A). While neither wild-type cells nor cells expressing only the *GAL2* permease gene (this strain is termed "GAL2") exhibit any growth inhibition from galactose, cells expressing the *GAL1* kinase gene (this strain is termed "GAL1") or both *GAL1* and *GAL2* exhibit sensitivity. The GAL1 strain exhibits lower sensitivity than the GAL1/2 strain, likely due to lower concentrations of substrate without expression of the galactose transporter. The observation of growth inhibition in the GAL1 strain is consistent with reports that some galactose enters the cells via general hexose transporters, which may critical for the activation of the galactose regulon in the appropriate conditions (Escalante-Chong *et al.*, 2015). Growth curves were repeated in both rich and minimal medium at 30° and 37°C and used to calculate inhibitory concentration values (Supplemental Figure 1 and Table 1). The GAL1/2 strain is roughly four to five times more sensitive to galactose than the GAL1 strain. Interestingly, both strains are roughly twofold more sensitive to galactose at 37°C compared with 30°C, but only in rich media; in minimal media, the IC_{50} values are the same regardless of growth temperature (Table 1).

Next we examined how Gal1P accumulation affects a number of growth parameters. Within 2 h (roughly one generation) of galactose addition, the GAL1/2 strain has stopped doubling and exhibits incomplete cell-cycle arrest in the G1/G0 stage of the cell cycle (Figure 2B). Cell volume steadily increases after cessation of growth (Figure 2B), indicating continued biomass production. Additionally, we observed that cell viability in growth inhibited cells remains high over 48 h (>50%) in a homozygous diploid version of the GAL1/2 strain (used to minimize suppressors that simply result from mutated *GAL1* and/or *GAL2* genes) (Figure 2C).

Because accumulation of some sugar-phosphate molecules, such as trehalose-6-phosphate, has been suggested to mediate heat sensitivity, we examined survival at 50°C 2 h after galactose addition. While both the wild-type and the GAL2 strain exhibit similar sensitivity to 50°C heat shock, the GAL1 and GAL1/2 strains exhibit better survival in a galactose-sensitivity-related manner (the GAL1/2 strain is more sensitive to galactose than the GAL1 strain and exhibits better survival than the GAL1 strain) (Figure 2D).

Strain	YPD (30°C)	YPD (37°C)	SD (30°C)	SD (37°C)
GAL1	1.05 (0.007)	0.53 (0.035)	0.85 (0.211)	0.98 (0.116)
GAL1/2	0.26 (0.007)	0.10 (0.001)	0.15 (0.002)	0.15 (0.001)
yrKHK	0.35 (0.013)	0.20 (0.003)	0.19 (0.004)	0.10 (0.005)

IC_{50} values indicate the concentration (percentage) at which growth rate is inhibited 50%; SD of two biological replicates for Gal1P (three biological replicates for Fru1P) is shown in parenthesis.

TABLE 1: IC_{50} for sugar-phosphate–accumulating strains.

Because the galactose-sensitive strains stop growing on exposure to galactose, and heat resistance is generally higher in quiescent cells compared to growing yeast, these experiments are insufficient to prove that Gal1P accumulation directly protects against heat.

We further examined whether Gal1P toxicity might result from specific metabolic blocks in fermentative or respiratory growth. *Saccharomyces cerevisiae* allows for facile distinction between the two possibilities. Mitochondrial petite (*rho*^{0}) versions of galactose-1-phosphate–accumulating strains, which can ferment glucose but not respire glucose, still exhibited sensitivity to galactose, suggesting that toxicity does not arise specifically from respiratory inhibition (Figure 2E). Further, Gal1P toxicity also occurs in cells grown on carbon sources that can be metabolized only by respiration (glycerol and ethanol), suggesting that toxicity does not arise specifically from inhibiting fermentative metabolic enzymes (Figure 2F).

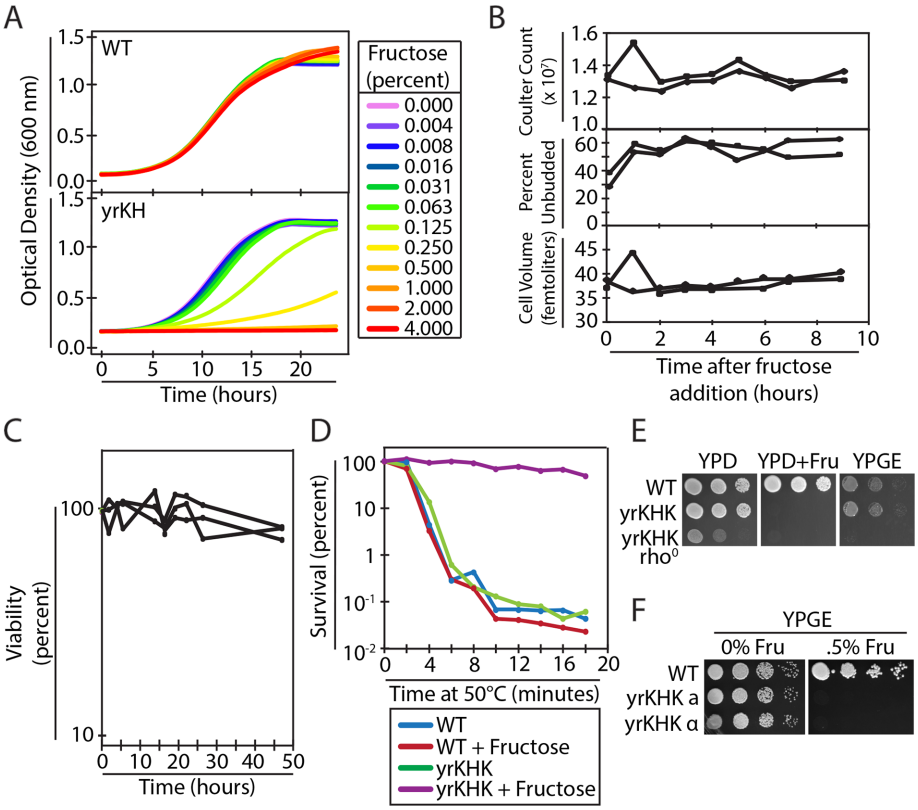

FIGURE 3: Physiological effects of fructose-1-phosphate accumulation. (A) Dose–response curves of indicated strains in YNB + 2% glucose at 30°C with indicated concentrations of fructose added (replicates and dose–response curves in different media are shown in Supplemental Figure 2). (B) yrKHK cells were grown to early log phase in YNB + 2% glucose before fructose was added to 2% at time zero. Cell volume and particle count were measured every hour with a Coulter counter. Percentage of unbudded cells was measured every hour with a hemocytometer. Each line represents an independent biological replicate. (C) yrKHK homozygous diploid cells were grown to early log phase in YNB + 2% glucose before fructose was added to 2% at time zero. Survival at indicated time points was assessed by plating and counting CFU on YPD plates. Each line represents an independent biological replicate. (D) Indicated strains were grown to log phase in YNB + 2% glucose before fructose was added to 2% for 2 h. Cells were then subjected to a 50°C heat shock, and samples were taken every 2 min and plated onto YPD to count CFU. (E) Tenfold serial dilutions of indicated strains were spotted onto YP medium containing either 2% glucose (YPD), 2% glucose and 2% fructose (YPD+Fru), or 3% glycerol and 2% ethanol (YPGE), as indicated. Cell density in initial spot was normalized to an OD_{600} = 1.0. Plates were incubated for 2 d at 30°C. (F) Tenfold serial dilutions of indicated strains were spotted onto YPGE plates containing indicated amounts of fructose. Cell density in initial spot was normalized to an OD_{600} = 1.0. Plates were incubated for 2 d at 30°C.

Physiological characterization of fructose-1-phosphate accumulation

Analogous growth curves were generated with the yrKHK strain to identify inhibitory concentrations of fructose in our system (Figure 3A and Supplemental Figure 2). Unlike Gal1P accumulation, however, the yrKHK strain exhibits roughly twofold higher sensitivity to fructose at higher temperatures in both rich and minimal media (Table 1). Fru1P accumulation also prevented growth within 2 h of addition, once again with incomplete cell cycle arrest at G1/G0 (Figure 3B). In contrast to Gal1P accumulation, yrKHK-expressing cells do not increase in volume over time, and exhibit even higher levels of survival over 48 h in a homozygous diploid version of the yrKHK strain (again, used to minimize suppressors that simply result from mutated yrKHK) (Figure 3, B and C). As observed with Gal1P accumulation, Fru1P accumulation results in better survival when challenged with a 50°C heat shock (Figure 3D). Further, Fru1P accumulation still prevented growth in strains unable to perform respiratory metabolism, or when grown using nonfermentable carbon sources (Figure 3, E and F).

Because yrKHK is an enzyme not normally found in yeast, we considered the possibility that Fru1P toxicity might result from localized Fru1P production. To examine the localization of this nonnative enzyme in yeast, we constructed a C-terminally tagged version using yeast-codon-optimized-EGFP,

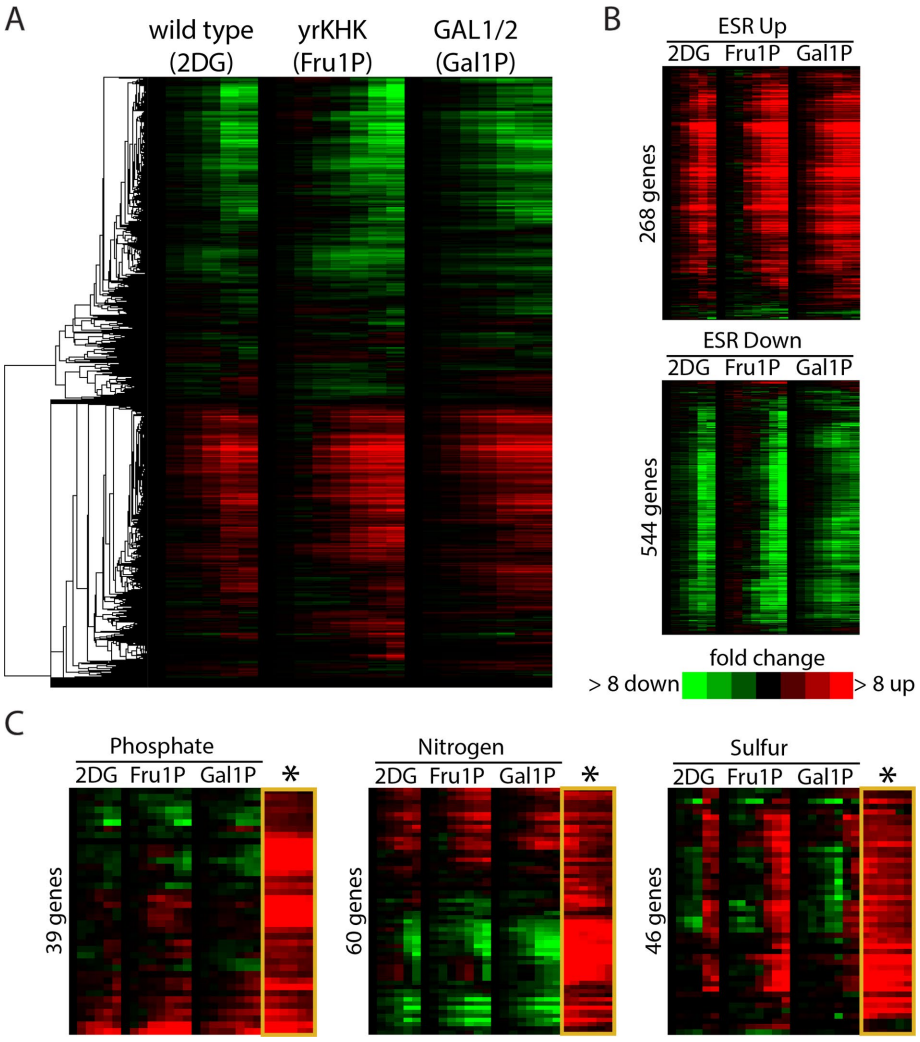

FIGURE 4: Gene expression response to sugar-phosphate accumulation. (A) Global view of clustered gene expression changes for 5438 yeast genes of the indicated strains in response to addition of the indicated sugars. Time-course sampling was performed as follows: for 2DG, 0, 2.5, 5, 10, 30, and 60 min; for both fructose and galactose, 0, 2.5, 5, 10, 15, 30, 60, and 120 min. (B) Gene expression response of environmental stress response (ESR) genes to each sugar-phosphate stress. (C) Gene expression response of nutrient-specific-limitation genes to each sugar-phosphate stress. Original gene expression response to nutrient limitation at different steady state growth rates from Brauer *et al.* is included in the yellow outlined box with an asterisk above (Brauer *et al.*, 2008). For B and C: as in A, gene expression data are from 2DG in wild type, fructose in yrKHK, and galactose in GAL1/2 (left to right). RNA extraction and microarray analysis were performed as described under *Materials and Methods*.

an enhanced variant of green fluorescent protein (Sheff and Thorn, 2004). This enzyme was still functional as measured by causing growth inhibition in the presence of fructose and had a diffuse localization throughout the cell, suggesting that toxicity was not due to localized Fru1P production (Supplemental Figure 3).

Gene expression response to sugar-phosphate accumulation

To examine transcriptional changes that result from sugar-phosphate accumulation, we performed time courses with the following conditions: wild-type cells with 2% 2-deoxyglucose (2DG), the yrKHK strain with 2% fructose, and the GAL1/2 strain with 2% galactose. 2DG has been used as an example of toxic sugar-phosphate accumulation, because after being phosphorylated to 6-phospho-2-deoxyglucose, it cannot be further converted to fructose-6-phosphate (Lobo and Maitra, 1977). We included it for comparison and used 2% as a concentration that provides complete arrest of cell division and results in similar physiological changes observed by Fru1P or Gal1P accumulation (Supplemental Figure 4). Samples were collected over a 2-h time course after adding the relevant toxicity-inducing sugar to each log-phase culture, and microarray analysis was performed to identify gene expression changes. As shown in Figure 4A, a large fraction of the genome exhibits gene expression changes, which are very similar among the different sugar-phosphate models.

To better understand these changes, we compared our expression data with groups of genes that respond to specific perturbations. In Figure 4B, we compared our gene expression data to the environmental stress response (ESR) (Gasch *et al.*, 2000). Gene expression changes in response to all three sugar-phosphates were largely coincident with the genes up- or down-regulated in response to environmental stress, which is also coincident with the set of genes that respond to slow growth (Brauer *et al.*, 2008). We did note that a few of the genes activated as part of the ESR are decreased in expression in response to sugar-phosphate and that a few genes that typically decrease expression as part of the ESR increase in response to sugar-phosphates (Figure 4B). Because ESR genes were defined by a typical response among a large panel of stress conditions, we sought to determine whether any specific environmental stressor affects gene expression similarly to these outlier genes in sugar-phosphate stress. The vast majority of these outlier genes (17 of 22) exhibit similar expression patterns in low-temperature growth conditions. We further compared our gene expression data to sets of genes that are activated in response to limitation of different nutrients, defined by Brauer *et al.* (2008). Of the genes highly expressed in response to phosphate-limitation, very few were activated in response to sugar-phosphate stress (Figure 4C). This suggests that in cells accumulating sugar-phosphates, intracellular phosphate is not limiting growth. Of the genes highly expressed in response to nitrogen limitation, some were also highly expressed by sugar-phosphate accumulation, while others were repressed (Figure 4C). Finally, of the genes activated in response to sulfur limitation, almost all were activated in a nonlinear manner (decreased transcripts at early time points, followed by induction at later time points) (Figure 4C). This suggests that some form of signaling similar to that of sulfur limitation is present in cells that accumulate certain sugar-phosphates. As part of this gene expression analysis, we also examined treatment with lower concentrations of inducing sugars, and the effect of galactose addition to the GAL2 strain, and observed few, if any, significant gene expression changes (Supplemental Figure 5).

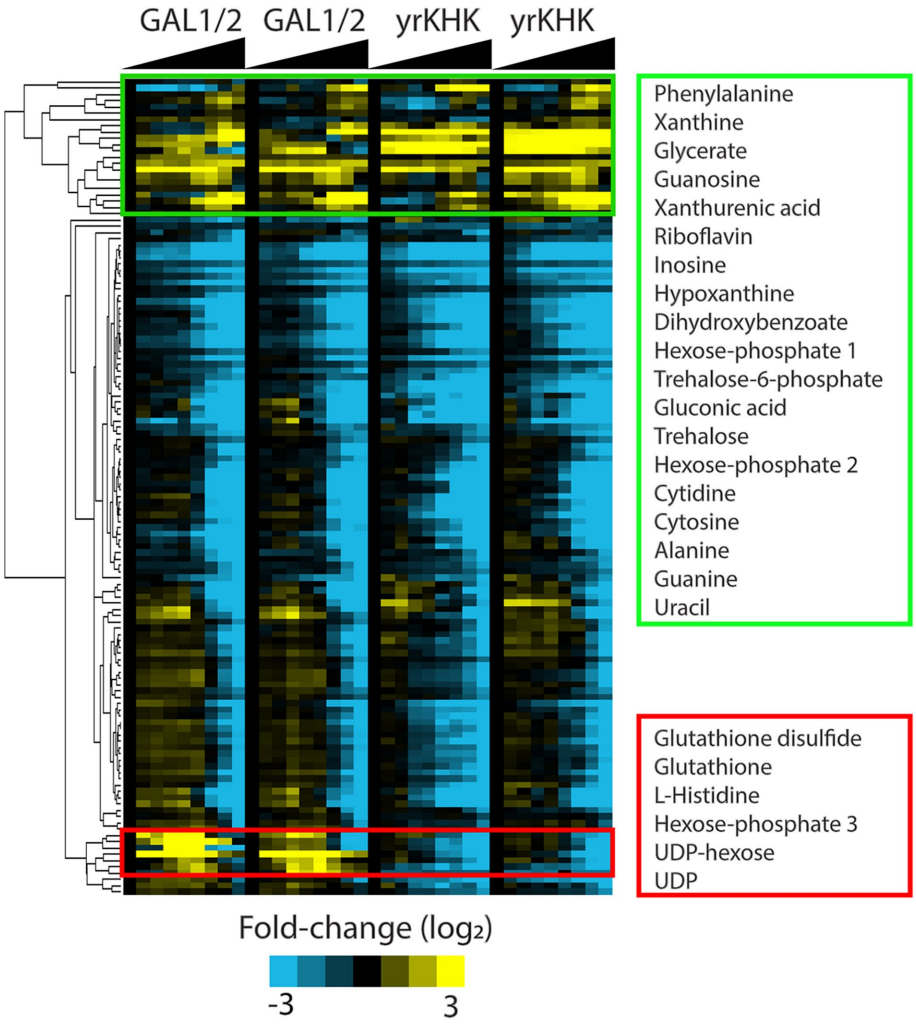

FIGURE 5: Metabolic response to sugar-phosphate toxicity. Indicated strains were grown to log phase in YNB + 1% glucose and then either galactose or fructose was added to 1% (wt/vol), respectively. Samples were taken for metabolite profiling at 0, 2.5, 5, 10, 15, 30, 60, 120, and 180 min. Metabolite profiling was performed as described under *Materials and Methods*. Two clusters of metabolites are highlighted and listed to the right of the heat-map. Shown are two biological duplicates for each strain.

Metabolic response to sugar-phosphate toxicity

While the gene expression responses to either Gal1P or Fru1P accumulation were highly similar, we also wanted to examine the metabolic impact of sugar-phosphate toxicity. We therefore examined the soluble metabolites extracted from either GAL1/2 or yrKHK in a 3-h time course after induction with either galactose or fructose, respectively. Metabolites were extracted and quantified by liquid chromatography tandem mass spectrometry (LC-MS). Of the 130 compounds we identified, the vast majority decrease in abundance as Gal1P and Fru1P accumulate and arrest cell division (Figure 5). In contrast, 19 of the compounds tend to increase in abundance along with the toxic sugar-phosphates. These compounds included trehalose and trehalose-6-phosphate, which typically rise when cell growth slows. They further include a number of nucleotide degradation products that typically rise in response to energy stress or RNA degradation (Figure 5). Taken together, these findings point to stalled, energy-stressed cells that are depleted of high-energy intermediates and accumulating lower energy waste products.

This basic pattern applies for both Gal1P or Fru1P. However, despite the similar patterns of metabolite changes in response to Gal1P or Fru1P, six compounds are notably different. These include glutathione and glutathione disulfide, UDP and UDP-hexose, and histidine, all of which increase when Gal1P but not Fru1P accumulates (Figure 5). While the underlying mechanism that causes these metabolic changes is unclear, it is tempting to speculate that the differential response in glutathione is related to the differential strength of induction of the sulfur starvation response genes. This provides another example of different cellular responses to accumulation of Gal1P or Fru1P.

Genetic suppressors of sugar-phosphate toxicity

To better understand the molecular mechanism of sugar-phosphate toxicity, we performed a number of genetic screens to look for random mutation suppressors of toxicity. A confounding issue in performing these classic genetic suppressor screens was loss-of-function mutations in toxicity-causing genes (*GAL1*, *GAL2*, or yrKHK). To rule out these mutations, each haploid suppressor was mated to a wild-type strain. Because these overexpression constructs are genetically dominant, loss-of-function mutations in toxicity-causing genes would still allow growth on toxicity-inducing sugars after crossing to a wild-type strain. In contrast, recessive suppressors in other genes would be complemented, and the functional toxicity-causing genes would still arrest growth. After crossing to a wild type, true dominant suppressors would also grow on toxicity-inducing sugars, therefore independent screens for dominant mutations were performed in strains that were homozygous for the toxicity-causing genes. To distinguish between true dominant suppression and mutations in both copies of toxicity-causing genes, potential suppressors were sporulated and tetrad analysis was performed using toxicity-causing medium. True dominant suppressors would segregate 2:2, whereas if both copies of a toxicity-causing gene were mutated, then all four spores would grow on toxicity-inducing medium.

After screening for recessive mutations to suppress Gal1P toxicity, over 70 independent suppressors were examined, and all had nonfunctional toxicity-causing genes (or dominant suppressors, though this is less likely). Additionally, 35 independent suppressors from a diploid strain homozygous for overexpressed *GAL1* and *GAL2* genes were examined for dominant suppressors. All appeared to have nonfunctional toxicity-causing genes using tetrad analysis as described above.

Twenty independent suppressors of Fru1P toxicity were examined, and 19 resulted from loss-of-function of yrKHK. The remaining strain appeared to contain a recessive suppressor mutation. This strain was back-crossed to a parent strain, and a number of suppressor and nonsuppressor progeny were pooled independently and sequenced. The most likely candidate mutation was a G-to-A transition mutation at –124 in the *ELF1* promoter region, which could

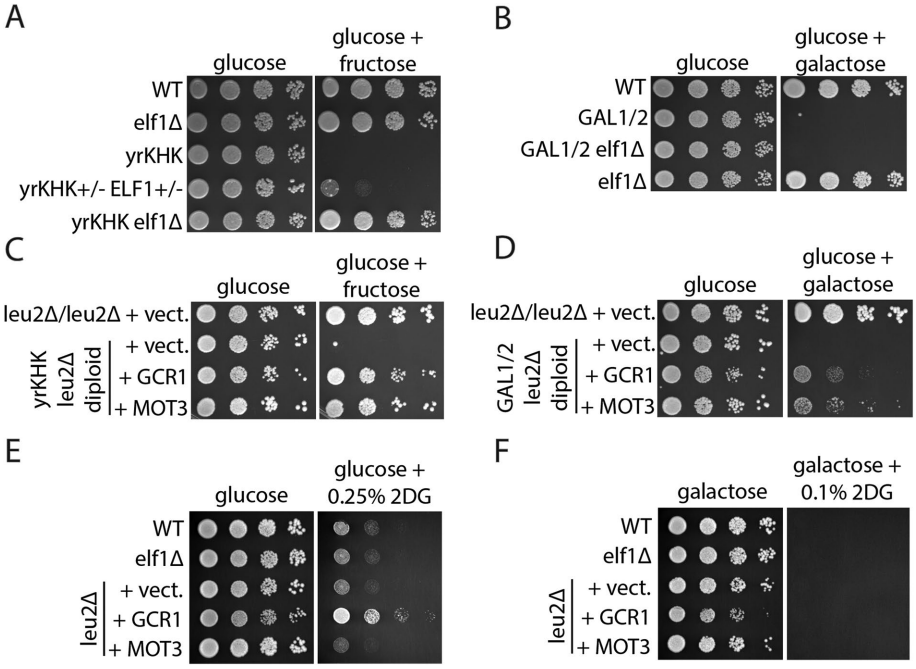

FIGURE 6: Genetic suppression of sugar-phosphate toxicity. (A–F) Tenfold serial dilutions of indicated strains were spotted onto YNB plates containing the indicated carbon sources (present at 2%, unless otherwise indicated). In C–F the parent vector used to express high copy suppressors was p425GPD. (A–D) Plates were incubated at 30°C for 2 d. (E, F) Plates were incubated at 30°C for 3 d.

potentially result in decreased levels of *ELF1* expression. *ELF1* encodes a protein involved in transcriptional elongation and chromatin structure maintenance (Prather *et al.*, 2005). Gene expression analysis of the suppressor strain confirmed that *ELF1* expression was lower in the suppressor mutant than in the parent strain (Supplemental Data). To confirm that loss of *ELF1* function causes suppression, the *ELF1* gene was independently deleted in the yrKHK strain. Removal of *ELF1* recapitulated the suppression observed in the original screen (Figure 6A). Even the heterozygous deletion appeared to result in some suppression, which aligns with the observation that decreased expression due to a promoter mutation could result in suppression (Figure 6A). Further, complementation of *elf1*Δ in the suppressed strain resulted in reversal of suppression (Supplemental Figure 6). As part of the *ELF1* complementation experiment, we observed that high levels of *ELF1* overexpression are mildly toxic (Supplemental Figure 6). Notably, *elf1*Δ does not suppress Gal1P toxicity (Figure 6B).

After screening for recessive mutations to suppress Fru1P toxicity, 27 independent suppressors from a diploid strain homozygous for yrKHK expression constructs were examined for dominant suppressors. All but one appeared to have nonfunctional yrKHK using tetrad analysis as described above. Genome sequencing of a backcrossed dominant suppressor revealed that the suppressor contained a mutation in yrKHK (C99R). This mutation lies in the conserved, dimerization interaction region of the ketohexokinase, which functions as a homodimer (Trinh *et al.*, 2009). This suggests that the C99R is a dominant negative allele that disrupts ketohexokinase function by interfering with dimerization (Supplemental Figure 7).

In addition to classic suppressor screens, we also used the barcoded MoBY 2.0 library to screen the GAL1/2 strain for overexpression suppressors (Magtanong *et al.*, 2011). The screen was performed in a diploid strain homozygous for overexpressed *GAL1*, *GAL2*, and for *leu2Δ0* that had been transformed with the *LEU2*$^+$ library. All suppressor colonies were pooled for barcode sequencing to identify potential suppressors. A number of potential suppressors were independently cloned and assessed. Only two genes were identified as true high-copy suppressors: *GCR1* and *MOT3*. *GCR1* encodes a transcriptional activator responsible for expression of glycolytic genes; loss of *GCR1* results in cells unable to perform glycolysis due to insufficient levels of glycolytic enzymes (Holland *et al.*, 1987; Lopez and Baker, 2000). *MOT3* also encodes a transcription factor involved in the repression and activation of various genes; additionally increased *MOT3* expression causes increased levels of the [MOT3$^+$] prion—a factor involved in cellular stress resistance (Grishin *et al.*, 1998; Madison *et al.*, 1998; Hongay *et al.*, 2002; Alberti *et al.*, 2009). Overexpression of either was sufficient to suppress both Gal1P and Fru1P toxicity, though suppression of Fru1P toxicity was more efficient (Figure 6, C and D). Further, overexpression of either *GCR1* or *MOT3* was able to restore growth to yrKHK when fructose was the only carbon source present, while neither overexpressed gene restored growth to GAL1/2 when galactose was the only carbon source present (Supplemental Figure 8).

We also examined these identified suppressors for the ability to suppress 2DG toxicity. Neither deletion of *ELF1* nor overexpression of *MOT3* was able to suppress 2DG toxicity (Figure 6E). In contrast, overexpression of *GCR1* was able to mildly suppress 2DG toxicity in glucose-containing medium, though suppression does not occur in galactose-containing medium (Figure 6F).

To determine whether these genetic suppressors ameliorated toxicity by simply decreasing the levels of toxic sugar-phosphates, we quantified sugar-phosphate accumulation in suppressor strains using an isotopic labeling strategy and LC-MS. Both Gal1P and Fru1P accumulated to an intracellular concentration of roughly 1 mM in the nonsuppressed strains (Figure 7). This is within the typical value observed for galactosemic patients after galactose ingestion, where Gal1P levels have been measured in red blood cells at concentrations ranging from 1 to 5 mM (Gitzelmann, 1995). Surprisingly, the suppressed strains did not have decreased levels of toxic sugar-phosphates. In contrast, *GCR1* overexpression suppressors increased the toxic sugar-phosphate levels by approximately two- to threefold (Figure 7, A and B). Overexpression of *MOT3* did not affect levels of Gal1P but did result in approximately twofold more Fru1P (Figure 7, A and B). Fru1P levels were also roughly doubled in the suppressor strain lacking *ELF1* (Figure 7C).

Nutritional supplementation fails to alleviate sugar-phosphate toxicity

One general hypothesis to explain the toxicity of sugar-phosphate accumulation is that cellular pools of phosphate are depleted. This seems unlikely, especially since cells stop dividing in less than 2 h despite the fact that yeast store large quantities of phosphate as polymers in their vacuoles (Ogawa *et al.*, 2000; Vagabov *et al.*, 2000). Furthermore, our gene expression analysis showed no sign of the typical phosphate-limitation response (Figure 4C). We tested this possibility in another way by adding exogenous phosphate to the medium and

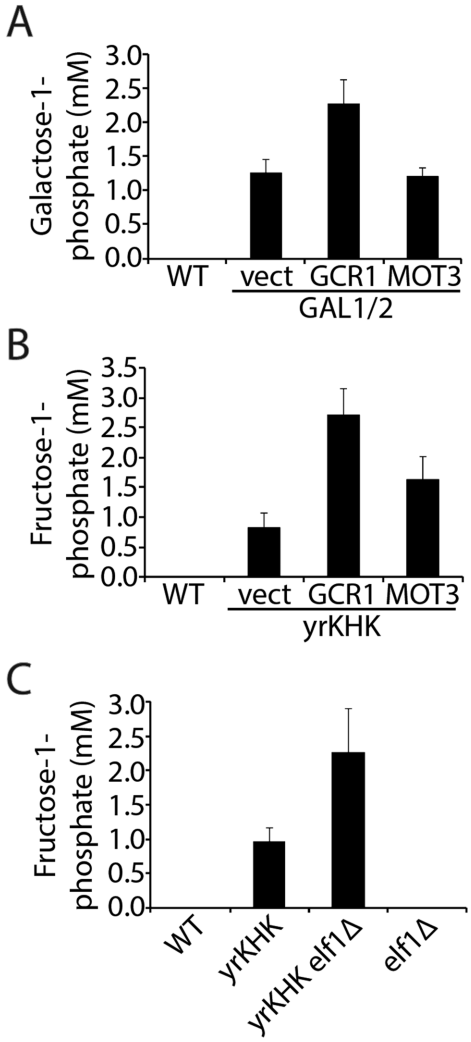

FIGURE 7: Genetic suppressors of sugar-phosphate toxicity do not decrease the levels of toxic sugar-phosphates. Labeled sugar-phosphate levels were quantified in the indicated strains after a 2-h treatment with the respective nonphosphorylated sugar. Metabolites were quantified as described under *Materials and Methods*. (A) Quantification of intracellular galactose-1-phosphate in GAL1/2 with and without overexpression suppressors. (B) Quantification of intracellular fructose-1-phosphate in yrKHK with and without overexpression suppressors. (C) Quantification of intracellular fructose-1-phosphate in yrKHK with and without *ELF1*. Error bars represent SD of three biological replicates.

observed no suppression of Gal1P or Fru1P toxicity (Supplemental Figure 9). Together, these data strongly suggest that depletion of phosphate pools is not the cause of sugar-phosphate toxicity.

Because our gene expression analysis indicated that genes expressed in response to limited methionine are being activated, we considered the possibility that sugar-phosphates might interfere with methionine biosynthesis. To test this possibility, we added exogenous methionine, or one of its biosynthetic products, the methyl donor *S*-adenosyl methionine (SAM), to the media. Neither methionine nor SAM suppressed Gal1P toxicity (Supplemental Figure 10). Another possibility included sugar-phosphate–mediated inhibition of the methionyl-tRNA synthetase enzyme, Mes1. To test this possibility, we overexpressed *MES1* and observed no suppression of Gal1P toxicity (Supplemental Figure 10).

Another hypothesis to explain the toxicity of sugar-phosphate accumulation is that sugar-phosphates are able to inhibit specific metabolic reactions. Because metabolic blocks can sometimes be remediated by supplementing nutrients after the blocked step, we also examined a number metabolic perturbations for the ability to suppress Gal1P toxicity. These included vitamin supplementation, metabolic intermediate supplementation, hypoxic growth in an anoxic chamber, and osmotic stabilization with sorbitol. None of these treatments suppressed Gal1P toxicity (Supplemental Figure 11). Further, standard rich medium contains an excess of many vitamins, amino acids, salts, and metals, yet both Gal1P and Fru1P are still toxic in this medium (Supplemental Figures 1 and 2).

DISCUSSION

In this study, we identify the common and divergent effects of sugar-phosphate accumulation on eukaryotic physiology using yeast as a model system. Standard ways of causing sugar-phosphate accumulation include mutations in genes that encode proteins that metabolize these intermediates further, confounding any toxic effect of the sugar-phosphate with the effect on the interruption of the metabolic pathways. Here we were able to isolate the toxic from the metabolic effects by arranging the accumulation of sugar-phosphates without interruption of the cognate metabolic pathway.

We observed that accumulation of either Gal1P or Fru1P results in rapid cessation of division, incomplete cell-cycle arrest, and minimal loss in viability. This does not appear to be a typical stress response, though, as these cells do not reach a new homeostasis and do not recover growth, even though they have the enzymatic means. Through analysis of the physiological changes associated with sugar-phosphate accumulation, and examination of genetic suppressors, we suggest that while there are common physiological effects of sugar-phosphate accumulation, toxicity likely results, at least in part, from interactions between different sugar-phosphates and multiple, distinct targets (e.g., Gal1P and Fru1P have multiple partially overlapping targets).

Physiological changes associated with sugar-phosphate accumulation

Typical starvation of yeast for a naturally limiting nutrient (glucose, phosphate, sulfate, etc.) results in over 90% arrest in the G1/G0 phase of the cell cycle, accompanied with high survival rates (Saldanha *et al.*, 2004; Boer *et al.*, 2008). Starvation of yeast for a nonnaturally limiting nutrient (leucine, uracil, etc.) results in incomplete cell-cycle arrest coupled with low survival rates (Saldanha *et al.*, 2004; Boer *et al.*, 2008). In contrast to either situation, accumulation of either Gal1P or Fru1P results in rapid growth arrest accompanied by incomplete cell cycle arrest, with high survival rates over 48 h. It is possible that survival rates would decrease over longer time spans; however, the experiment is technically challenging as suppressor mutations occur frequently enough to cause overgrowth even in a diploid background.

Growth arrest associated with Gal1P, Fru1P, or 2DG accumulation results in a gene expression response indicative of stressed cells by comparison to the ESR. The same result was observed using the *gal7*Δ-based model of galactosemia in yeast (Slepak *et al.*, 2005). The gene expression response to sugar-phosphate accumulation, especially among genes induced by sulfur or nitrogen limitation, is suggestive of a metabolic perturbation in the cell, though it remains unclear exactly what changes occur and are being sensed. Furthermore, Gal1P- and Fru1P-mediated growth arrest correlates with increased thermotolerance. Both these

observations are in agreement with data demonstrating that slow growth elicits the ESR and results in thermotolerance (Brauer *et al.*, 2008; Lu *et al.*, 2009).

In contrast to these similarities, we also observed a number of physiological differences associated with specific sugar-phosphates. For example, sensitivity to Gal1P in minimal medium is the same at both 30° and 37°C, while sensitivity to Fru1P is increased at 37°C. Additionally, after growth arrest, Gal1P-accumulating cells continue to increase in cell volume, while Fru1P-accumulating cells do not. Gal1P accumulation also causes some intracellular metabolites to increase in the cell, while this is not the case for Fru1P. Further, our results demonstrate that neither Gal1P nor Fru1P accumulation results in thermosensitivity at 50°C (instead both treatments result in thermotolerance). This is in contrast to the 50°C thermosensitivity observed in *tps2*Δ cells, which accumulate trehalose-6-phosphate (Piper and Lockheart, 1988; van Vaeck *et al.*, 2001). Thus, either thermosensitivity of *tps2*Δ is not due to trehalose-6-phosphate accumulation per se but rather due to other physiological changes associated with disruption of trehalose biosynthesis, or, alternatively, trehalose-6-phosphate interacts with a unique target to mediate thermosensitivity.

Taken together, the physiological data suggest that while there are some common characteristics of cells that have accumulated sugar-phosphates, there are also a number of differences. These differences suggest at least some nonoverlapping targets for unique sugar-phosphate isomers.

Genetic suppressors of sugar-phosphate toxicity

A screen for high-copy suppressors of Gal1P toxicity identified both *GCR1* and *MOT3*. While neither gene is conserved in humans, both genes encode transcriptional regulators of metabolism and functional homologues likely exist. Both genes are able to suppress Gal1P and Fru1P toxicity; only *GCR1* suppresses 2DG toxicity and only slightly. Variability between suppression is also suggestive that each type of sugar-phosphate has at least some different targets. Identification of metabolic regulators, rather than individual biosynthetic enzymes, suggests that each sugar-phosphate has multiple targets and requires large-scale metabolic remodeling to overcome inhibition.

While a classic suppressor screen failed to find any suppressor mutations of Gal1P toxicity, we did identify two suppressor mutations of Fru1P toxicity. One was a dominant mutation in yrKHK itself (C99R). The other was a loss-of-function mutation in the transcription elongation factor *ELF1*, a highly conserved gene (ELOF1 in humans). It remains unclear why *ELF1* deletion suppresses Fru1P toxicity, and it is equally interesting and unclear why *elf1*Δ does not suppress Gal1P or 2DG toxicity. One explanation for *elf1*Δ suppression would be coincident induction of high-copy suppressor genes; this appears to not be the case in the original suppressor strain (comparing suppressor strain expression to the parent yrKHK strain: *GCR1* is 1.7-fold down, *MOT3* is 1.1-fold down, and *PMU1* is unchanged). Together, variability of suppression activity suggests that each type of sugar-phosphate has different targets.

The apparent simplest way to bypass toxicity associated with sugar-phosphate levels would be to remove the sugar-phosphates (by removing the phosphate with a phosphatase, transporting the sugar-phosphates out of the cell, etc.). Surprisingly, the suppressors identified as part of this work either increase sugar-phosphate levels or do not affect the sugar-phosphate levels at all. Further work is required to uncover the molecular mechanisms that drive the suppression activity described here.

Comparison to other sugar-phosphate toxicity models

Previous work has also identified a number of genes whose overexpression suppresses galactose sensitivity in galactosemic yeast models. These include overexpression of human myo-inositol monophosphatase (hIMP1), UDP-glucose pyrophosphorylase (*UGP1*), and aldose reductase (*GRE3*) (Mehta *et al.*, 1999; Lai and Elsas, 2000; Masuda *et al.*, 2008). We assessed whether these suppressors have any role in our models of Gal1P, Fru1P, or 2DG toxicity. We recapitulated suppression of Gal1P toxicity by overexpression of either yeast inositol monophosphatase (*INM1* or *INM2*) (Supplemental Figure 12). In both cases, suppression is likely a result of hexose-phosphatase activity on the toxic Gal1P. However, neither *UGP1* nor *GRE3* overexpression were able to suppress Gal1P toxicity in our model. Both suppressors were identified using the *gal7*Δ model of galactosemia, which blocks conversion of Gal1P to Glu1P (and also blocks concomitant synthesis of UDP-galactose from UDP-glucose). This suggests that these suppressors may result from interaction with other aspects of the *gal7*Δ perturbation, instead of the direct consequences of Gal1P accumulation. Neither Fru1P toxicity nor 2DG toxicity were suppressed by any of these Gal1P overexpression suppressors. Mild suppression of Fru1P toxicity was observed after overexpression of *PMU1*, a putative phosphomutase shown to suppress temperature sensitivity of a *tps2*Δ strain (Elliott *et al.*, 1996). Suppression of *tps2*Δ heat sensitivity by *PMU1* overexpression was hypothesized to result from phosphomutase action directly causing the observed decrease in trehalose-6-phosphate levels (Elliott *et al.*, 1996). This would likely be the case for Fru1P and 2DG as well.

Additionally, suppressors of 2DG toxicity have also been described. Some of these suppressors, such as loss-of-function mutations in hexokinases (which prevent sugar-phosphate formation) and altered sugar transport (which likely prevents uptake of 2DG) do not provide information regarding the molecular mechanism of phosphorylated 2DG toxicity (Lobo and Maitra, 1977; Novak *et al.*, 1990). Others have identified genes involved in glucose sensing and signaling such as *HXK2*, *REG1*, *GLC7*, *GRR1*, and *SNF1* (Zimmermann and Scheel, 1977; Entian, 1980; Neigeborn and Carlson, 1987; McCartney *et al.*, 2014). Given that the majority of 2DG toxicity suppressors are involved in glucose transport, sensing, and signaling, this molecule not only results in sugar-phosphate accumulation but also directly interferes with glucose signaling and metabolism. For these reasons, 2DG may not be an ideal model to study the direct effects of sugar-phosphate accumulation.

Open questions

Despite rapid growth arrest associated with Gal1P or Fru1P, cells are able to resume normal growth promptly when plated onto rich medium. A sugar-phosphate–specific lag time is observed within the first culture doubling after removal of the toxicity-inducing sugar, followed by normal division times (Supplemental Figure 13). How the cells detoxify the accumulated sugar-phosphate molecules remains unclear. Additionally, specific targets of individual sugar-phosphate molecules remain to be identified. Perhaps most importantly, it remains to be determined whether lessons learned from investigating sugar-phosphate toxicity in yeast will be relevant to understanding human genetic diseases or, even more tantalizingly, diet-induced metabolic syndrome.

MATERIALS AND METHODS

Yeast media

Yeast cell growth and standard laboratory manipulations were performed as described (Guthrie and Fink, 2002). All media used was either minimal medium (YNB; 0.67% yeast nitrogen base without

amino acids plus 2% indicated carbon sources) or rich medium (YP; 2% bacto peptone, 1% yeast extract, 2% indicated carbon sources). Exceptions are noted in the text (for example, YPGE medium contained 2% bacto peptone, 1% yeast extract, 3% glycerol, and 2% ethanol). Additionally, for fluorescence microscopy, low-fluorescence medium was used (standard minimal medium with 2% glucose, except YNB is prepared without riboflavin or folic acid to reduce background fluorescence) (Sheff and Thorn, 2004).

Yeast growth

Culture growth was measured either using a Klett Colorimeter (Manostat Corporation) of 25- to 50-ml cultures in 250-ml Klett flasks or using a Synergy H1 Hybrid reader (BioTek) with 200-µl cultures in a 96-well plate (plate was sealed with a Breathe-Easy gas-permeable membrane from Research Products International Corporation). Measurements of cell density were also performed by measuring absorbance at 600 nm using a Genesys 6 spectrophotometer (Thermo Scientific). Measurements of cell density and volume were also performed using a Coulter Z2 Particle Count and Size Analyzer (Beckman Coulter) with a 50-µm aperture. Bud index (percentage unbudded) was counted using a hemocytometer—at least 300 cells were counted for each sample. For comparative growth assays, cells were spotted onto relevant media. This involved dilution of a culture to an OD_{600} of 1.0, followed by 10-fold serial dilutions. All dilutions were then spotted onto solid media using a Replica Plater for 96-well Plate, 8 × 6 array (Sigma-Aldrich).

Yeast strain construction

All strains were made in the DBY12000 background (Table 2). Most gene deletions were made by transformation into a diploid to produce a heterozygote, which was confirmed by PCR and then dissected to get MAT**a** and MATα segregants. The *TDH3*$_{pr}$-yrKHK construct was generated by PCR, inserted into a haploid strain, confirmed by PCR, and then backcrossed to wild type to isolate MAT**a** and MATα segregants. All combinatorial gene deletion/insertion strains were made by mating, sporulating, and tetrad dissection. Sporulation

Strain	Name in text	Genotype	Reference
DBY12000	WT	MAT**a** prototrophic *HAP1*$^{+}$ derivative of FY4	Hickman and Winston, 2007[a]
DBY12106	GAL1	MAT**a** *gal1*$_{pr}$(-5 to -583)Δ::kanMX-*TDH3*$_{pr}$(-1 to -680)	This study
DBY12107	GAL2	MATα *gal2*$_{pr}$(-5 to -528)Δ::natAC[b]-*TDH3*$_{pr}$(-1 to -680)	Gibney *et al.*, 2015
DBY12130	GAL1/2	MAT**a** *gal1*$_{pr}$Δ::kanMX-*TDH3*$_{pr}$ *gal2*$_{pr}$Δ::natAC[b]-*TDH3*$_{pr}$	This study
DBY12549	yrKHK	MAT**a** *can1*Δ::*TDH3*$_{pr}$-yrKHK	This study
DBY12569	GAL1/2 diploid	*gal1*$_{pr}$Δ::kanMX-*TDH3*$_{pr}$/*gal1*$_{pr}$Δ::kanMX-*TDH3*$_{pr}$ *gal2*$_{pr}$Δ::natAC[b]-*TDH3*$_{pr}$/*gal2*$_{pr}$Δ::natAC[b]-*TDH3*$_{pr}$	This study
DBY12316	WT *rho*^{0}	MAT**a** *rho*^{0} (derived from DBY12000)	This study
DBY12319	GAL1 *rho*^{0}	MAT**a** *gal1*$_{pr}$Δ::kanMX-*TDH3*$_{pr}$ *rho*^{0}	This study
DBY12322	GAL2 *rho*^{0}	MAT**a** *gal2*$_{pr}$Δ::natAC-*TDH3*$_{pr}$ *rho*^{0}	This study
DBY12325	GAL1/2 *rho*^{0}	MAT**a** *gal1*$_{pr}$Δ::kanMX-*TDH3*$_{pr}$ *gal2*$_{pr}$Δ::natAC[b]-*TDH3*$_{pr}$ *rho*^{0}	This study
DBY12570	yrKHK diploid	*can1*Δ::*TDH3*$_{pr}$-*yrKHK/can1*Δ::*TDH3*$_{pr}$-*yrKHK*	This study
DBY12746	yrKHK *rho*^{0}	MAT**a** *can1*Δ::*TDH3*$_{pr}$-yrKHK *rho*^{0}	This study
DBY12695	*elf1*Δ	MAT**a** *elf1*Δ::natAC[b]	This study
DBY12707	yrKHK *elf1*Δ	MAT**a** *can1*Δ::*TDH3*$_{pr}$-yrKHK *elf1*Δ::natAC[b]	This study
DBY12743	GAL1/2 *elf1*Δ	MAT**a** *gal1*$_{pr}$Δ::kanMX-*TDH3*$_{pr}$ *gal2*$_{pr}$Δ::bleMX-*TDH3*$_{pr}$ *elf1*Δ::natAC	This study
DBY12045	*ura3*Δ	MAT**a** *ura3Δ0*	This study
DBY12756	yrKHK *ura3*Δ	MAT**a** *can1*Δ::*TDH3*$_{pr}$-*yrKHK ura3Δ0*	This study
DBY12758	yrKHK *elf1*Δ *ura3*Δ	MAT**a** *can1*Δ::*TDH3*$_{pr}$-yrKHK *elf1*Δ::natAC[b] *ura3Δ0*	This study
DBY12691	yrKHK-C99R	MAT**a** *can1*Δ::*TDH3*$_{pr}$-yrKHK-C99R; dominant negative allele of yrKHK (original isolated suppressor strain)	This study
DBY12374	*leu2*Δ/*leu2*Δ	*leu2Δ0/leu2Δ0*	This study
DBY12557	yrKHK *leu2*Δ diploid	*can1*Δ::*TDH3*$_{pr}$-*yrKHK/can1*Δ::*TDH3*$_{pr}$-*yrKHK leu2Δ0/leu2Δ0*	This study
DBY12373	GAL1/2 *leu2*Δ diploid	*gal1*$_{pr}$Δ::*kanMX-TDH3*$_{pr}$/*gal1*$_{pr}$Δ::*kanMX-TDH3*$_{pr}$ *gal2*$_{pr}$Δ::*natAC*[b]-*TDH3*$_{pr}$/*gal2*$_{pr}$Δ::*natAC*[b]-*TDH3*$_{pr}$ *leu2Δ0/leu2Δ0*	This study
DBY12344	GAL1/2 *ura3*Δ	*gal1*$_{pr}$Δ::kanMX-*TDH3*$_{pr}$ *gal2*$_{pr}$Δ::natAC[b]-*TDH3*$_{pr}$ *ura3Δ0*	This study
DBY12578	MAT**a** yrKHK-yEGFP	MAT**a** *can1*Δ::*TDH3*$_{pr}$-yrKHK-yEGFP-kanMX	This study
DBY12579	MATα yrKHK-yEGFP	MATα *can1*Δ::*TDH3*$_{pr}$-yrKHK-yEGFP-kanMX	This study

[a]This strain is a GAL^{+}, prototrophic derivative of S288C. The details for construction of this strain are found in Hickman and Winston (2007), while the first article using this strain is Hickman *et al.* (2011). The strain was a kind gift from the Winston lab (where it is named FY2648).
[b]natAC refers to a version of the natMX dominant drug resistance marker cassette that contains a yeast codon-optimized *nat*^{r} gene. This cassette was a kind gift from Amy Caudy (University of Toronto).

TABLE 2: Strains used in this study.

Strain	Plasmid name	Restriction sites	Reference
RB3620	p416GPD		Mumberg *et al.*, 1995
RB3587	p416GPD-*ELF1*	*Spe*I-*ELF1*-*Xho*I	This study
RB3621	p426GPD		Mumberg *et al.*, 1995
RB3588	p426GPD-*ELF1*	*Spe*I-*ELF1*-*Xho*I	This study
RB3570	p426GPD-*MES1*	*Spe*I-*MES1*-*Xho*I	This study
RB3622	p425GPD		Mumberg *et al.*, 1995
RB3601	p425GPD-*GCR1*	*Spe*I-*GCR1*-*Xho*I	This study
RB3597	p425GPD-*MOT3*	*Spe*I-*MOT3*-*Xho*I	This study
RB3407	p426GPD-*INM1*	*Spe*I-*INM1*-*Xho*I	This study
RB3408	p426GPD-*UGP1*	*Spe*I-*UGP1*-*Xho*I	This study
RB3411	p426GPD-*GRE3*	*Spe*I-*GRE3*-*Xho*I	This study
RB3412	p426GPD-*INM2*	*Spe*I-*INM2*-*Xho*I	This study
RB3414	p426GPD-*PMU1*	*Spe*I-*PMU1*-*Xho*I	This study

TABLE 3: Plasmids used in this study.

was performed by growing cells to log phase in rich media, collecting cells by centrifugation, washing once in 1% potassium acetate, and then resuspending in 1% potassium acetate. Cells were then incubated at room temperature on a roller wheel for at least 4 d before tetrad dissection. Petite (rho^0) strains were generated as described (Guthrie and Fink, 2002). Briefly, cells were passaged in YNB + 2% glucose + 25 µg/ml EtBr twice before being plated onto YPD. Single colonies were screened for loss of mitochondrial DNA using both inability to grow on nonfermentable carbon sources (YPGE) and PCR for a number of mitochondrial genes (*Q0010*, *OLI1*, and *COX3*).

Plasmid construction

Plasmids were built using pRS-series shuttle vector backbones (Sikorski and Hieter, 1989; Mumberg *et al.*, 1995). Inserted genes were amplified using PCR primers from Integrated DNA Technologies (IDT) containing the indicated restriction sites incorporated into their sequence (Table 3). After ligation and transformation, individual colonies were screened for correct insertion using restriction digest. Sanger sequencing was further used to confirm insertion of the correct gene in at least one clone identified as correct by restriction digest (using the Genewiz sequencing service).

Genetic suppressor screens

Classic screens for spontaneous suppressor mutations. All screens were performed by growing independent cultures overnight in YNB + 2% glucose medium, followed by plating onto toxicity-inducing medium (YNB + 2% glucose and 2% galactose for GAL1/2, YNB + 2% glucose, and 2% fructose for yrKHK). For each independent culture, ~10^7 cells were spread onto a single plate then incubated for 3–4 d at 30°C. Suppression due to mutations affecting the toxicity-causing genes was ruled out as described under *Results*. For the two suppressors identified using classic genetic screens, both were backcrossed to produce a pool of suppressing and nonsuppressing segregants. Pools were combined then sequenced in an Illumina HiSeq 2500, aligned to a reference *S. cerevisiae* genome using SAMtools (Li *et al.*, 2009), and potential variants were identified using freebayes (Garrison and Marth, 2012). All potential variants were manually examined in Integrative Genomics Viewer (Robinson *et al.*, 2011; Thorvaldsdóttir *et al.*, 2013).

High-copy suppressor screen. A diploid strain homozygous for overexpressed *GAL1* and *GAL2*, and for *leu2Δ0*, was used for the high-copy suppressor screen. This strain was transformed with the *LEU2*$^+$, barcoded MoBY 2.0 plasmid library (a kind gift from the Charlie Boone lab, University of Toronto) (Magtanong *et al.*, 2011). Approximately 32,000 independent transformants were pooled together, and ~200,000 cells from this pool were plated onto each of 15 YNB + 2% glucose and 2% galactose plates. All suppressor colonies were then pooled together for plasmid extraction. Plasmid barcodes were amplified using PCR on the extracted population of plasmids. The barcodes were then sequenced in an Illumina HiSeq 2500, and then barcodes were mapped to genes as previously described (Gibney *et al.*, 2013). The 10 most abundant genes were tested for suppression by independently cloning the identified genes into a different high-copy plasmid (p425GPD).

Assessment of thermotolerance

To assess thermotolerance, cells were grown to log phase in minimal media. Multiple 0.5-ml aliquots were removed from the culture into microcentrifuge tubes. For the heat shock, tubes were immersed in a 50°C water bath for 0, 2, 4, 6, 8, 10, 12, 14, 16, 18, or 20 min and then chilled on ice for the remaining duration of the time course (we measured that it takes less than 1 min for 0.5 ml of 30°C culture to reach 50°C in the water bath). Cells were plated on rich media to count viable colony forming units (CFU).

RNA extraction, microarrays, and gene expression analysis

For gene expression analysis using microarrays, samples were collected for RNA extraction by vacuum filtration onto nylon filters. Filters were immediately placed into tubes, submerged into liquid nitrogen, and stored at –80°C until RNA extraction. RNA was extracted by the acid-phenol method and cleaned using RNeasy mini columns (Qiagen). RNA was amplified and labeled using the Agilent Quick Amp Labeling Kit (Agilent Technologies). The reference RNA for all samples was taken as the experimental time-zero point. Cy5-labeled experimental cRNA was mixed with the Cy3-labeled reference cRNA in equal proportions and hybridized for 17 h at 60°C to a custom Agilent yeast microarray (AMADID 017566). Microarrays were washed and then scanned with an Agilent DNA microarray scanner (Agilent Technologies). Agilent Feature Extraction software was used to extract intensity data. Resulting microarray intensity data were submitted to the PUMA Database (http://puma.princeton.edu) for archiving and analysis. Features flagged as outliers due to low intensity or poor quality were excluded from further analysis. All data with intensity values less than 350 were set to 350 to prevent overestimating large fold changes due to fluctuations of small numbers. Genes missing data at any time-point were also excluded. Each time-series experiment was zero-normalized before hierarchical clustering was performed (Pearson uncentered metric, average linkage) using Cluster 3.0 (http://bonsai.hgc.jp/~mdehoon/software/cluster/). Nonnormalized time-zero data were also compared to confirm that no significant changes were present (Supplemental Figure 5). Data were visually represented, examined, and exported using Java TreeView version 1.1.6r2 (http://jtreeview.sourceforge.net/). Data are available for download in the Supplemental Data.

For comparison of gene expression changes in response to sugar-phosphate accumulation, previously published data were obtained and used. For comparison to genes that increase or decrease in transcript level as part of the ESR, the data presented in Figure 3 of

Gasch *et al.* (2000) were downloaded from http://genome-www.stanford.edu/yeast_stress/. Our gene expression data were then mapped onto those sets of genes; for genes present in the ESR data, but missing in our data set, the gene was removed from analysis. For comparison to genes that have increased expression in response to specific nutrient limitations, the entire data set from Brauer *et al.* (2008) was downloaded from http://growthrate.princeton.edu/. Hierarchical clustering was performed (Pearson uncentered metric, average linkage) using Cluster 3.0, and nutrient-specific clusters were selected and exported using Java TreeView version 1.1.6r2. Our gene expression data were then mapped onto those sets of genes. Expression data for each exported cluster is also shown in a yellow box to the right of the sugar-phosphate gene expression data (data are ordered as in Brauer *et al.*, 2008, where gene expression from left to right corresponds to changing steady-state growth rates from slow to fast: 0.05, 0.1, 0.15, 0.2, 0.25, 0.3 per hour).

Metabolite profiling

For metabolomic profiling, ~7.5×10^7 cells were collected at each time point, filtered onto a nylon membrane, and quenched by placing the filter into an 80:20 mixture of HPLC-grade methanol and high-performance liquid chromatography (HPLC)-grade water at –20°C. This was allowed to chill at –20°C for at least 20 min. Then, the resulting slurry of extraction solvent and cell debris was repeatedly pipetted over the filter (to collect any residual material stuck to the filter) and collected into a microcentrifuge tube. The slurry was centrifuged at 4°C for 5 min, and a fraction of this supernatant was dried under nitrogen gas for resuspension and metabolite profiling using -MS on Thermo Scientific Vanquish UPLCs and Q Exactive Plus Mass spectrometers. Each sample was examined using two different analytical methods.

Method 1 used negative-mode ionization with a tributylamine ion pairing method using an Agilent Zorbax RRHD Extend C18 column (2.1 × 150 mm, 1.8 µm particles) (Lu *et al.*, 2008, 2010; Crutchfield *et al.*, 2010). Mobile phase A was 10 mM tributylamine, 15 mM acetic acid in 97:3 water:methanol; mobile phase B was methanol and a flow rate of 0.2 ml/min was used. The column was equilibrated for 4 min in 0% B prior to injection, followed by a gradient of 0% B from 0 to 2.5 min, 20% B at 5 min, 20% B from 5 to 7.5 min, 55% B at 13 min, 95% B at 15 min, 95% B from 15 to 18.5 min, 0% B at 19, and 0% B from 19 to 22 min. The source parameters were as follows: Sheath gas: 30; Aux gas:12; Sweep gas: 0; spray voltage –3.0 kV; capillary temperature of 320°C; S-lens RF level of 55. The mass spectrometer was operated in data-dependent top-6 MS^2 mode, with 70,000 resolution setting and AGC of 3e6 for MS^1 and 17,500 resolution setting and AGC target of 1e6 for MS^2. Stepped, normalized collision energies of 20, 50, and 100 were used.

Method 2 used positive-mode ionization with separation on a SeQuant ZIC-pHILIC column (150 × 2.1 mm, 5-µm polymer particles) (Lu *et al.*, 2008, 2010; Crutchfield *et al.*, 2010; Zhang *et al.*, 2012). Mobile phase A was water with 20 mM NH_4CO_3, pH 9.2, with ammonium hydroxide; mobile phase B was acetonitrile, and a flow rate of 0.15 ml/min was used. The column was equilibrated for 6 min in 80% B prior to injection, followed by a gradient of 80–20% B from 0 to 20 min, 15% B at 22 min, 80% B at 22.5 min, and 80% B from 22.5 to 24 min. The source parameters were as follows: Sheath gas: 40; Aux gas:15; Sweep gas: 1; spray voltage 3.1 kV, capillary temperature of 275°C, and S-lens RF level of 50. The mass spectrometer was operated in data-dependent top-6 MS^2 mode, with 70,000 resolution setting and AGC of 3e6 for MS^1, and 17,500 resolution setting and AGC target of 1e5 for MS^2. Stepped, normalized collision energies of 20, 40, and 80 were used.

Data were then analyzed using the open-source software Metabolomic Analysis and Visualization ENgine (Melamud *et al.*, 2010). Compounds were identified by comparison against an in-house generated database of metabolite fragmentation patterns and retention times. Peak height data for identified compound are available in the Supplemental Data.

Sugar-phosphate quantification

For quantification of sugar-phosphate molecules, samples were grown in minimal medium containing 1% (wt/vol) uniformly labeled ^{13}C-glucose (Cambridge Isotopes) to early exponential phase at 30°C. A time-zero sample was taken for metabolite profiling as described above. Next, either 1,2-^{13}C galactose (Cambridge Isotopes) or 1,2-^{13}C fructose (Cambridge Isotopes) was added to each culture to a final concentration of 1% (wt/vol). After 2 h, samples were taken for metabolite extraction. Sample were prepared as described above, and the dried metabolite samples were resuspended in HPLC-grade water containing 5 µg/ml (wt/vol) either unlabeled galactose-1-phosphate (Sigma-Aldrich) or fructose-1-phosphate (BOC Sciences). Sugar-phosphate levels were measured using method 1 as described above. Concentrations were calculated by determining the ratio of peak areas for the endogenously produced 1,2-^{13}C-labeled peak and the unlabeled standard peak from the same injection. This experimental design avoids inaccurate quantification due to other potentially confounding hexose phosphates present in yeast cells. The intracellular concentration of each sugar-phosphate was calculated assuming an average cell volume of 45 fl.

Fluorescence microscopy

Strains were grown in low-fluorescence medium with 2% glucose to early log phase, and then an aliquot was removed and fixed in 10% formaldehyde for 15 min at room temperature before being washed in phosphate-buffered saline with 0.5% Tween-20 (PBS-T). For the remainder of the culture, fructose was added to 2%, and cells were incubated at 30°C on a roller wheel for 1 h before fixation. All samples were suspended in Prolong Gold with 4,6-diamino-2-phenylindole (DAPI) (Life Technologies) before imaging.

All images were taken using an IX81 inverted fluorescence microscope (Olympus) with a motorized stage (Prior), PlanApo TIRFM 100× oil objective with a numerical aperture of 1.45, X-Cite Exacte light source (EXFO), IX2-SHA motorized shutter, and ORCA II ER Mono charge-coupled device (CCD) camera (Hamamatsu). Images were acquired using Slidebook 5.0 digital image acquisition software (Intelligent Imaging Innovations). Cells were imaged using DIC optics and a 50-ms exposure. DAPI staining was imaged with a DAPI filter and a 200-ms exposure. GFP was imaged using a fluorescein isothiocyanate (FITC) filter and a 200-ms exposure. At least 10 images were taken for each strain; shown in the figure is a representative image (Supplemental Figure 3).

ACKNOWLEDGMENTS

We thank members of the Rose, Gammie, and Botstein labs for helpful discussion. We also thank Wei Wang, Donna Storton, Jessica Buckles, Lance Parsons, and Dave Robinson for assistance with Illumina sequencing and analysis. This research was supported by the National Institute of General Medical Sciences Center for Quantitative Biology (GM071508), a National Institutes of Health grant to D.B. (GM046406), a Department of Energy grant to J.R. (DE-SC0012461), and National Institutes of Health grants to P.G. (GM097852) and Calico Life Sciences LLC.

REFERENCES

Alberti S, Halfmann R, King O, Kapila A, Lindquist S (2009). A systematic survey identifies prions and illuminates sequence features of prionogenic proteins. Cell 137, 146–158.

Boer VM, Amini S, Botstein D (2008). Influence of genotype and nutrition on survival and metabolism of starving yeast. Proc Natl Acad Sci USA 105, 6930–6935.

Botstein D, Fink GR (2011). Yeast: an experimental organism for 21st century biology. Genetics 189, 695–704.

Brauer MJ, Huttenhower C, Airoldi EM, Rosenstein R, Matese JC, Gresham D, Boer VM, Troyanskaya OG, Botstein D (2008). Coordination of growth rate, cell cycle, stress response, and metabolic activity in yeast. Mol Biol Cell 19, 352–367.

Crutchfield CA, Lu W, Melamud E, Rabinowitz JD (2010). Mass spectrometry-based metabolomics of yeast. Methods Enzymol 470, 393–426.

de Jongh WA, Bro C, Ostergaard S, Regenberg B, Olsson L, Nielsen J (2008). The roles of galactitol, galactose-1-phosphate, and phosphoglucomutase in galactose-induced toxicity in Saccharomyces cerevisiae. Biotechnol Bioeng 101, 317–326.

De-Souza EA, Pimentel FSA, Machado CM, Martins LS, da-Silva WS, Montero-Lomelí M, Masuda CA (2014). The unfolded protein response has a protective role in yeast models of classic galactosemia. Dis Model Mech 7, 55–61.

Donaldson IA, Doyle TC, Matas N (1993). Expression of rat liver ketohexokinase in yeast results in fructose intolerance. Biochem J 291(Pt 1), 179–186.

Douglas HC, Hawthorne DC (1964). Enzymatic expression and genetic linkage of genes controlling galactose utilization in Saccharomyces. Genetics 49, 837–844.

Doyle TC, Spickett CM, Donaldson IA, Ratcliffe RG (1993). Metabolic studies of a fructose-intolerant yeast by in vivo 31P-nuclear magnetic resonance spectroscopy. Yeast 9, 867–873.

Elliott B, Haltiwanger RS, Futcher B (1996). Synergy between trehalose and Hsp104 for thermotolerance in Saccharomyces cerevisiae. Genetics 144, 923–933.

Englesberg E, Anderson RL, Weinberg R, Lee N, Hoffee P, Huttenhauer G, Boyer H (1962). L-Arabinose-sensitive, L-ribulose 5-phosphate 4-epimerase-deficient mutants of Escherichia coli. J Bacteriol 84, 137–146.

Entian KD (1980). Genetic and biochemical evidence for hexokinase PII as a key enzyme involved in carbon catabolite repression in yeast. Mol Gen Genet 178, 633–637.

Escalante-Chong R, Savir Y, Carroll SM, Ingraham JB, Wang J, Marx CJ, Springer M (2015). Galactose metabolic genes in yeast respond to a ratio of galactose and glucose. Proc Natl Acad Sci USA 112, 1636–1641.

Froesch ER (1969). Disorders of fructose metabolism. J Clin Pathol Suppl (Ass Clin Path) 2, 7–12.

Fukasawa T, Nikaido H (1959). Galactose-sensitive mutants of Salmonella. Nature 184(Suppl), 1168–1169.

Gammie AE, Erdeniz N, Beaver J, Devlin B, Nanji A, Rose MD (2007). Functional characterization of pathogenic human MSH2 missense mutations in Saccharomyces cerevisiae. Genetics 177, 707–721.

Garrison E, Marth G (2012). Haplotype-based variant detection from short-read sequencing. arXiv:1207.3907.

Gasch AP, Spellman PT, Kao CM, Carmel-Harel O, Eisen MB, Storz G, Botstein D, Brown PO (2000). Genomic expression programs in the response of yeast cells to environmental changes. Mol Biol Cell 11, 4241–4257.

Gibney PA, Schieler A, Chen JC, Rabinowitz JD, Botstein D (2015). Characterizing the in vivo role of trehalose in Saccharomyces cerevisiae using the AGT1 transporter. Proc Natl Acad Sci USA 1506289112-.

Gibney PA, Lu C, Caudy AA, Hess DC, Botstein D (2013). Yeast metabolic and signaling genes are required for heat-shock survival and have little overlap with the heat-induced genes. Proc Natl Acad Sci USA 110, E4393–E4402.

Gitzelmann R (1995). Galactose-1-phosphate in the pathophysiology of galactosemia. Eur J Pediatr 154(Suppl 2), S45–S49.

Grishin AV, Rothenberg M, Downs MA, Blumer KJ (1998). Mot3, a Zn finger transcription factor that modulates gene expression and attenuates mating pheromone signaling in Saccharomyces cerevisiae. Genetics 149, 879–892.

Guthrie C, Fink GR (2002). Guide to yeast genetics and molecular and cell biology. Cell 2009, 600.

Herman RH, Zakim D (1968). Fructose metabolism. IV. Enzyme deficiencies: essential fructosuria, fructose intolerance, and glycogen-storage disease. Am J Clin Nutr 21, 693–698.

Hickman MJ, Petti AA, Ho-Shing O, Silverman SJ, McIsaac RS, Lee TA, Botstein D (2011). Coordinated regulation of sulfur and phospholipid metabolism reflects the importance of methylation in the growth of yeast. Mol Biol Cell 22, 4192–4204.

Hickman MJ, Winston F (2007). Heme levels switch the function of Hap1 of Saccharomyces cerevisiae between transcriptional activator and transcriptional repressor. Mol Cell Biol 27, 7414–7424.

Holland MJ, Yokoi T, Holland JP, Myambo K, Innis MA (1987). The GCR1 gene encodes a positive transcriptional regulator of the enolase and glyceraldehyde-3-phosphate dehydrogenase gene families in Saccharomyces cerevisiae. Mol Cell Biol 7, 813–820.

Hongay C, Jia N, Bard M, Winston F (2002). Mot3 is a transcriptional repressor of ergosterol biosynthetic genes and is required for normal vacuolar function in Saccharomyces cerevisiae. EMBO J 21, 4114–4124.

Jin YS, Ni H, Laplaza JM, Jeffries TW (2003). Optimal growth and ethanol production from xylose by recombinant Saccharomyces cerevisiae require moderate D-xylulokinase activity. Appl Environ Microbiol 69, 495–503.

Kadner RJ, Murphy GP, Stephens CM (1992). Two mechanisms for growth inhibition by elevated transport of sugar phosphates in Escherichia coli. J Gen Microbiol 138, 2007–2014.

Lai K, Elsas LJ (2000). Overexpression of human UDP-glucose pyrophosphorylase rescues galactose-1-phosphate uridyltransferase-deficient yeast. Biochem Biophys Res Commun 271, 392–400.

Lai K, Elsas LJ, Wierenga KJ (2009). Galactose toxicity in animals. IUBMB Life 61, 1063–1074.

Lai K, Langley SD, Khwaja FW, Schmitt EW, Elsas LJ (2003). GALT deficiency causes UDP-hexose deficit in human galactosemic cells. Glycobiology 13, 285–294.

Lang GI, Parsons L, Gammie AE (2013). Mutation rates, spectra, and genome-wide distribution of spontaneous mutations in mismatch repair deficient yeast. G3 GeneslGenomeslGenetics 3, 1453–1465.

Li H, Handsaker B, Wysoker A, Fennell T, Ruan J, Homer N, Marth G, Abecasis G, Durbin R (2009). The sequence alignment/map format and SAMtools. Bioinformatics 25, 2078–2079.

Lobo Z, Maitra PK (1977). Resistance to 2-deoxyglucose in yeast: a direct selection of mutants lacking glucose-phosphorylating enzymes. Mol Gen Genet 157, 297–300.

Lopez MC, Baker HV (2000). Understanding the growth phenotype of the yeast gcr1 mutant in terms of global genomic expression patterns. J Bacteriol 182, 4970–4978.

Lu C, Brauer MJ, Botstein D (2009). Slow growth induces heat-shock resistance in normal and respiratory-deficient yeast. Mol Biol Cell 20, 891–903.

Lu W, Bennett BD, Rabinowitz JD (2008). Analytical strategies for LC-MS-based targeted metabolomics. J Chromatogr B Anal Technol Biomed Life Sci 871, 236–242.

Lu W, Clasquin MF, Melamud E, Amador-Noguez D, Caudy AA, Rabinowitz JD (2010). Metabolomic analysis via reversed-phase ion-pairing liquid chromatography coupled to a stand alone orbitrap mass spectrometer. Anal Chem 82, 3212–3221.

Lyngstadaas A, Sprenger GA, Boye E (1998). Impaired growth of an Escherichia coli rpe mutant lacking ribulose-5-phosphate epimerase activity. Biochim Biophys Acta 1381, 319–330.

Madison JM, Dudley AM, Winston F (1998). Identification and analysis of Mot3, a zinc finger protein that binds to the retrotransposon Ty long terminal repeat (delta) in Saccharomyces cerevisiae. Mol Cell Biol 18, 1879–1890.

Magtanong L *et al.* (2011). Dosage suppression genetic interaction networks enhance functional wiring diagrams of the cell. Nat Biotechnol 29, 505–511.

Masuda CA, Previato JO, Miranda MN, Assis LJ, Penha LL, Mendonça-Previato L, Montero-Lomelí M (2008). Overexpression of the aldose reductase GRE3 suppresses lithium-induced galactose toxicity in Saccharomyces cerevisiae. FEMS Yeast Res 8, 1245–1253.

McCartney RR, Chandrashekarappa DG, Zhang BB, Schmidt MC (2014). Genetic analysis of resistance and sensitivity to 2-deoxyglucose in Saccharomyces cerevisiae. Genetics 198, 635–646.

Mehta DV, Kabir A, Bhat PJ (1999). Expression of human inositol monophosphatase suppresses galactose toxicity in Saccharomyces cerevisiae: Possible implications in galactosemia. Biochim Biophys Acta 1454, 217–226.

Melamud E, Vastag L, Rabinowitz JD (2010). Metabolomic analysis and visualization engine for LC-MS data. Anal Chem 82, 9818–9826.

Mumberg D, Muller R, Funk M (1995). Yeast vectors for the controlled expression of heterologous proteins in different genetic backgrounds. Gene 156, 119–122.

Neigeborn L, Carlson M (1987). Mutations causing constitutive invertase synthesis in yeast: genetic interactions with snf mutations. Genetics 115, 247–253.
Novak S, D'Amore T, Stewart GG (1990). 2-Deoxy-D-glucose resistant yeast with altered sugar transport activity. FEBS Lett 269, 202–204.
Ogawa N, DeRisi J, Brown PO (2000). New components of a system for phosphate accumulation and polyphosphate metabolism in Saccharomyces cerevisiae revealed by genomic expression analysis. Mol Biol Cell 11, 4309–4321.
Petry KG, Reichardt JKV (1998). The fundamental importance of human galactose metabolism: Lessons from genetics and biochemistry. Trends Genet 14, 98–102.
Piper PW, Lockheart A (1988). A temperature-sensitive mutant of Sacchromyces cerevisiae defective in the specific phosphatase of trehalose biosynthesis. FEMS Microbiol Lett 49, 245–250.
Prather D, Krogan NJ, Emili A, Greenblatt JF, Winston F (2005). Identification and characterization of Elf1, a conserved transcription elongation factor in Saccharomyces cerevisiae. Mol Cell Biol 25, 10122–10135.
Robinson JT, Thorvaldsdóttir H, Winckler W, Guttman M, Lander ES, Getz G, Mesirov JP (2011). Integrative genomics viewer. Nat Biotechnol 29, 24–26.
Rodriguez-Pena JM, Cid VJ, Arroyo J, Nombela C (1998). The YGR194c (XKS1) gene encodes the xylulokinase from the budding yeast Saccharomyces cerevisiae. FEMS Microbiol Lett 162, 155–160.
Saldanha AJ, Brauer MJ, Botstein D (2004). Nutritional homeostasis in batch and steady-state culture of yeast. Mol Biol Cell 15, 4089–4104.
Sheff MA, Thorn KS (2004). Optimized cassettes for fluorescent protein tagging in Saccharomyces cerevisiae. Yeast 21, 661–670.
Sikorski RS, Hieter P (1989). A system of shuttle vectors and yeast host strains designed for efficient manipulation of DNA in Saccharomyces cerevisiae. Genetics 122, 19–27.
Sirr A, Cromie GA, Jeffery EW, Gilbert TL, Ludlow CL, Scott AC, Dudley AM (2015). Allelic variation, aneuploidy, and nongenetic mechanisms suppress a monogenic trait in yeast. Genetics 199, 247–262.
Slepak T, Tang M, Addo F, Lai K (2005). Intracellular galactose-1-phosphate accumulation leads to environmental stress response in yeast model. Mol Genet Metab 86, 360–371.
Thorvaldsdóttir H, Robinson JT, Mesirov JP (2013). Integrative Genomics Viewer (IGV): high-performance genomics data visualization and exploration. Brief Bioinform 14, 178–192.
Trinh CH, Asipu A, Bonthron DT, Phillips S EV (2009). Structures of alternatively spliced isoforms of human ketohexokinase. Acta Crystallogr D 65, 201–211.
van Vaeck C, Wera S, van Dijck P, Thevelein JM (2001). Analysis and modification of trehalose 6-phosphate levels in the yeast Saccharomyces cerevisiae with the use of Bacillus subtilis phosphotrehalase. Biochem J 353, 157–162.
Vagabov VM, Trilisenko LV, Kulaev IS (2000). Dependence of inorganic polyphosphate chain length on the orthophosphate content in the culture medium of the yeast Saccharomyces cerevisiae. Biochemistry (Mosc) 65, 349–354.
Yarmolinsky MB, Wiesmeyer H, Kalckar HM, Jordan E (1959). Hereditary defects in galactose metabolism in Escherichia coli mutants, II. Galactose-induced sensitivity. Proc Natl Acad Sci USA 45, 1786–1791.
Zhang T, Creek DJ, Barrett MP, Blackburn G, Watson DG (2012). Evaluation of coupling reversed phase, aqueous normal phase, and hydrophilic interaction liquid chromatography with orbitrap mass spectrometry for metabolomic studies of human urine. Anal Chem 84, 1994–2001.
Zimmermann FK, Scheel I (1977). Mutants of Saccharomyces cerevisiae resistant to carbon catabolite repression. Mol Gen Genet 154, 75–82.